Published November 19, 2012

Csi1 links centromeres to the nuclear envelope for centromere clustering

Haitong Hou,[1] Zhou Zhou,[2] Yu Wang,[1] Jiyong Wang,[1] Scott P. Kallgren,[1] Tatiana Kurchuk,[1] Elizabeth A. Miller,[1] Fred Chang,[2] and Songtao Jia[1]

[1]Department of Biological Sciences; and [2]Department of Microbiology and Immunology, Columbia University College of Physicians and Surgeons; Columbia University, New York, NY 10027

In the fission yeast *Schizosaccharomyces pombe*, the centromeres of each chromosome are clustered together and attached to the nuclear envelope near the site of the spindle pole body during interphase. The mechanism and functional importance of this arrangement of chromosomes are poorly understood. In this paper, we identified a novel nuclear protein, Csi1, that localized to the site of centromere attachment and interacted with both the inner nuclear envelope SUN domain protein Sad1 and centromeres. Both Csi1 and Sad1 mutants exhibited centromere clustering defects in a high percentage of cells. Csi1 mutants also displayed a high rate of chromosome loss during mitosis, significant mitotic delays, and sensitivity to perturbations in microtubule–kinetochore interactions and chromosome numbers. These studies thus define a molecular link between the centromere and nuclear envelope that is responsible for centromere clustering.

Introduction

Eukaryotic genomic DNA is folded with histone and nonhistone proteins into chromatin, which is then arranged into complex higher-order structures to achieve the level of compaction needed to fit the entire genome into the nucleus. It is increasingly recognized that spatial and temporal genome organization is essential for gene expression, DNA replication, and maintenance of genome stability (Misteli, 2007; Mekhail and Moazed, 2010; Meister et al., 2011; Rajapakse and Groudine, 2011). One of the most striking examples of genome organization is the Rabl-like configuration of chromosomes in the interphase nuclei, in which centromeres are clustered at the nuclear periphery. This clustering has been seen in diverse cell types ranging from yeast, to plants, to flies (Funabiki et al., 1993; Jin et al., 1998; Fang and Spector, 2005).

The centromere is a specialized region of DNA within every chromosome that directs the assembly of the kinetochore, which is essential for the attachment of spindle microtubules to drive chromosome segregation during mitosis (Cheeseman and Desai, 2008; Verdaasdonk and Bloom, 2011). In interphase fission yeast cells, chromosomes are attached by their centromeres to the inner nuclear envelope near the region of the spindle pole body (SPB; centrosome equivalent; Funabiki et al., 1993). The SPB is cytoplasmic but near the nuclear envelope at this cell cycle stage (Ding et al., 1997). During mitosis, the SPBs insert into the nuclear envelope and then nucleate microtubules inside the nucleus for spindle assembly (Ding et al., 1997). The centromeres are released from the nuclear envelope and then recaptured by these intranuclear microtubules, which subsequently align and segregate the chromosomes for mitosis (Funabiki et al., 1993).

Little is known about the molecular details of how the centromeres are clustered and attached to the inner nuclear envelope near the SPB during interphase. This interphase chromosomal arrangement is dependent on kinetochore proteins but is independent of microtubules or pericentric heterochromatin (Funabiki et al., 1993; Ding et al., 1997; Appelgren et al., 2003; Castagnetti et al., 2010). Mutations of *mis6* (inner kinetochore component) and *nuf2* (outer kinetochore Ndc80 complex component) result in centromere declustering (Appelgren et al., 2003; Asakawa et al., 2005), but how kinetochore components are linked to the nuclear envelope near the SPB remains unknown. SUN domain protein Sad1 and KASH domain proteins Kms1/2 are excellent candidates, as these are nuclear envelope proteins that concentrate in the vicinity of the SPB, at the site of

Y. Wang, J. Wang, and S.P. Kallgren contributed equally to this paper.

Correspondence to Songtao Jia: jia@biology.columbia.edu

Abbreviations used in this paper: ChIP, chromatin immunoprecipitation; EMM, Edinburgh minimal medium; SAC, spindle assembly checkpoint; SPB, spindle pole body.

Supplemental Material can be found at:
http://jcb.rupress.org/content/suppl/2012/11/15/jcb.201208001.DC1.html

The Rockefeller University Press $30.00
J. Cell Biol. Vol. 199 No. 5 735–744
www.jcb.org/cgi/doi/10.1083/jcb.201208001

Published November 19, 2012

centromere clustering (Starr and Fischer, 2005; Razafsky and Hodzic, 2009; Mekhail and Moazed, 2010). SUN/KASH domain proteins have conserved roles in linking cytoplasmic structures, such as centrosomes and actin filaments, to nuclear structures, including chromosomes in many cell types (Starr and Fischer, 2005; Razafsky and Hodzic, 2009; Mekhail and Moazed, 2010). Sad1 and Kms1 have been shown to mediate telomere clustering in meiosis (Chikashige et al., 2006), but their functions in interphase centromere clustering have not been tested.

Several other genes have been reported to affect interphase centromere clustering, including *crm1*, *mto1*, *nsk1*, and *ima1* (Funabiki et al., 1993; Franco et al., 2007; King et al., 2008; Buttrick et al., 2011; Hiraoka et al., 2011). Crm1 is an essential protein involved in nuclear–cytoplasmic protein transport (Fukuda et al., 1997), making analysis of its role in regulating centromere clustering difficult. *mto1Δ* and *nsk1Δ* only produce mild defects in centromere clustering, and these proteins do not localize to SPB–kinetochore during interphase (Franco et al., 2007; Buttrick et al., 2011; Chen et al., 2011), making them likely to act indirectly on this process. The role of Ima1 in SPB–kinetochore interactions is controversial (King et al., 2008; Hiraoka et al., 2011). Here, we identify a novel protein, Csi1, that plays a major role in centromere clustering. Moreover, Csi1 interacts with Sad1 and centromere components and thus may serve as a critical link between centromeres and the nuclear envelope.

Results and discussion

To identify novel factors required for proper chromosome segregation, we screened a fission yeast haploid deletion library for mutants that affect the maintenance of nonessential minichromosome Ch16 (Niwa et al., 1986). Cells that lose Ch16 appeared red when grown on low adenine medium, and mutations that affect chromosome segregation resulted in a mixture of white and red cells (Fig. 1 A). One of the strongest defects was observed in the deletion of an uncharacterized ORF, SPBC2G2.14, which we named *csi1*$^+$ (*chromosome segregation impaired protein 1*; Fig. 1 A).

We found that *csi1Δ* cells have a strong defect in centromere clustering. We assayed kinetochore behavior by imaging inner kinetochore protein Mis6-GFP (homologue of mammalian CENP-I) and Cnp20-GFP (homologue of mammalian CENP-T). In wild-type interphase cells, all three centromeres were clustered at the site of the SPB, marked by Sid4-mRFP (Figs. 1 B and S1 A; Chang and Gould, 2000). These kinetochore markers appeared as multiple dots (at most three) in the nucleus in *csi1Δ* cells during interphase, indicated by a single unduplicated SPB or by cytosolic microtubules (Figs. 1, B and C; and S1 A). This phenotype was corroborated by the high incidence of *cen2*-GFP delocalization from Sid4-mRFP in *csi1Δ* cells (Fig. S1 C).

Because centromere clustering requires functional kinetochores (Appelgren et al., 2003), we examined the effect of *csi1Δ* on kinetochore structures. Loss of Csi1 had no effect on the association of kinetochore proteins, such as Mis6, Cnp1, and Cnp20, to centromeric DNA as assayed by chromatin immunoprecipitation (ChIP) analysis (Figs. 1 D and S1 B) and by live-cell imaging (Figs. 1 B and S1 A). Moreover, the characteristic micrococcal nuclease digestion pattern of centromeric chromatin (Takahashi et al., 1992) is not affected in *csi1Δ* cells (unpublished data). Thus, these layers of the kinetochore appear largely intact in *csi1Δ* cells.

To determine the localization of Csi1, we generated yeast strains expressing GFP- or mCherry-tagged versions of Csi1 at its native chromosomal location. Live-cell imaging revealed that Csi1 was concentrated at a single spot near the nuclear periphery in interphase cells, where the centromeres are clustered near the SPB as indicated by GFP-tagged centromeric proteins, such as Cnp1 and Mis6 (Fig. 2 A), or mRFP-tagged SPB protein Sid4 (Fig. 2 E). ChIP analysis revealed that Csi1 associates with centromeric DNA and is enriched at the *cnt* region, upon which the kinetochore assembles, but not the surrounding pericentric heterochromatin (Fig. 2, B and C). In mutants of inner (*cnp1-1* and *mis6-302*) and outer (*mis12-537* and *nuf2-degron*) kinetochore components, Csi1 dissociated from centromeres as assayed by ChIP (Figs. 2 D and S2, A–C).

Csi1 also colocalized with the SUN domain protein Sad1, which is localized on the nuclear envelope near the SPB. Time-lapse microscopy revealed that Csi1 colocalized with Sad1-DsRed near or at the SPB throughout interphase and mitosis and separated from centromeres (marked by Mis6-GFP) during mitosis, when the centromeres are released (Fig. S2 D). In the kinetochore mutants *cnp1-1* or *mis6-302* at a restrictive temperature, Csi1-GFP still localized to a single dot that colocalized with the SPB component Sid4 (Figs. 2 E and S2 E), suggesting that Csi1 can localize to the vicinity of the SPB independently of kinetochores.

We next showed that a *sad1.1* mutant (Hagan and Yanagida, 1995) also caused centromere declustering. In this temperature-sensitive *sad1* mutant, Csi1-GFP was localized in a diffuse nuclear pattern at restrictive temperature, suggesting that Csi1 depends on Sad1 for localization (Fig. 2 F). The delocalization of Csi1 and declustering of centromeres were prominent by 90 min after temperature shift (unpublished data). As the *sad1.1* mutant predominantly blocks the cell cycle at the second cell division after temperature shift (Hagan and Yanagida, 1995), the early appearance of centromere declustering is unlikely the result of a cell cycle block at M phase. In contrast, *csi1Δ* has no effect on Sad1 localization to the SPB (Fig. S1 D).

We probed whether Csi1 interacts with Sad1 and kinetochore components using immunoprecipitation analysis and found that Csi1 interacted with Sad1 and a kinetochore component Spc7 (homologue of mammalian KNL1; Fig. 2 G). ChIP analyses showed that Sad1 was detectable at centromeres in a Csi1-dependent manner (Fig. 2 H). These data suggest that Sad1 and Csi1 are part of the molecular link between the nuclear envelope and the centromeres (Fig. 2 I).

Csi1 encodes a sequence orphan without predicted membrane association domains. Through constructing a series of Csi1 deletions at its endogenous chromosomal locus, we found that an N-terminal segment (2–29 aa) was required for correct Csi1 localization to the SPB (Fig. 3 A). Deletion of this segment of Csi1 (Δ2–29 aa) resulted in diffuse Csi1-GFP signal within

Published November 19, 2012

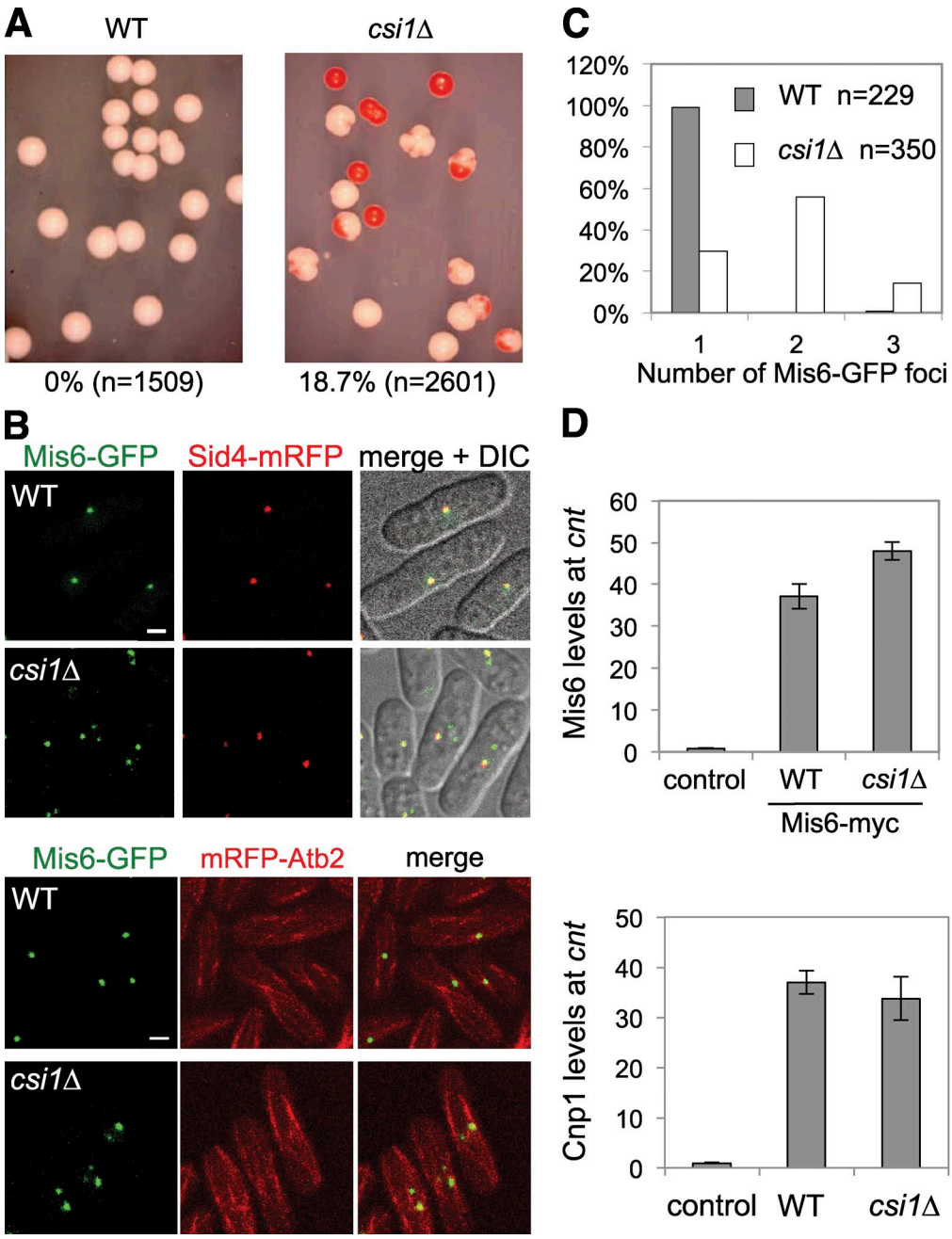

Figure 1. **Csi1 is required for centromere clustering during interphase.** (A) Cells containing Ch16 were grown as single colonies to measure chromosome loss rate, shown below each picture. *n* indicates total number of colonies counted. (B) Live-cell imaging of Mis6-GFP in wild-type and *csi1Δ* cells. Sid4-mRFP and mRFP-Atb2 were used to confirm that cells are at interphase. (C) Quantification of the number of Mis6 foci in interphase cells. *n* represents the number of cells counted from a single experiment. (D) ChIP analysis of Mis6 and Cnp1 levels at centromeres (*cnt*). Error bars represent standard deviations of three experiments. DIC, differential interference contrast; WT wild type. Bars, 1 µm.

the nucleus and abolished Csi1 association with centromeres (Fig. 3, B, C, and F). Because this phenotype was similar to that seen in the *sad1.1* mutant, we tested whether this domain is required for Sad1 interaction. Yeast two-hybrid and coimmunoprecipitation analysis demonstrated that full-length Csi1 interacted with Sad1, and this interaction was abolished in Csi1-(Δ2–29) (Fig. 3, D and E). We also substituted two leucines with prolines (Csi1-2LP; L199P and L209P) at the endogenous *csi1*$^{+}$ chromosome locus to disrupt a predicted coiled coil (Fig. 3 A). Csi1-2LP abolished the interaction between Csi1 and kinetochores as indicated by both ChIP and coimmunoprecipitation analyses (Fig. 3, C and F). However, this mutant form of Csi1 still interacts with the SPB as indicated by both imaging and coimmunoprecipitation analyses (Fig. 3, B and E). These data suggest that proper targeting of Csi1 to the SPB is required for Csi1 association with kinetochores, possibly with the help of additional proteins near the SPB. As expected, both the *Δ2–29* and *2LP* mutants showed defects in centromere clustering and minichromosome maintenance to a degree similar to that of *csi1Δ* (Fig. 3, G and H).

Published November 19, 2012

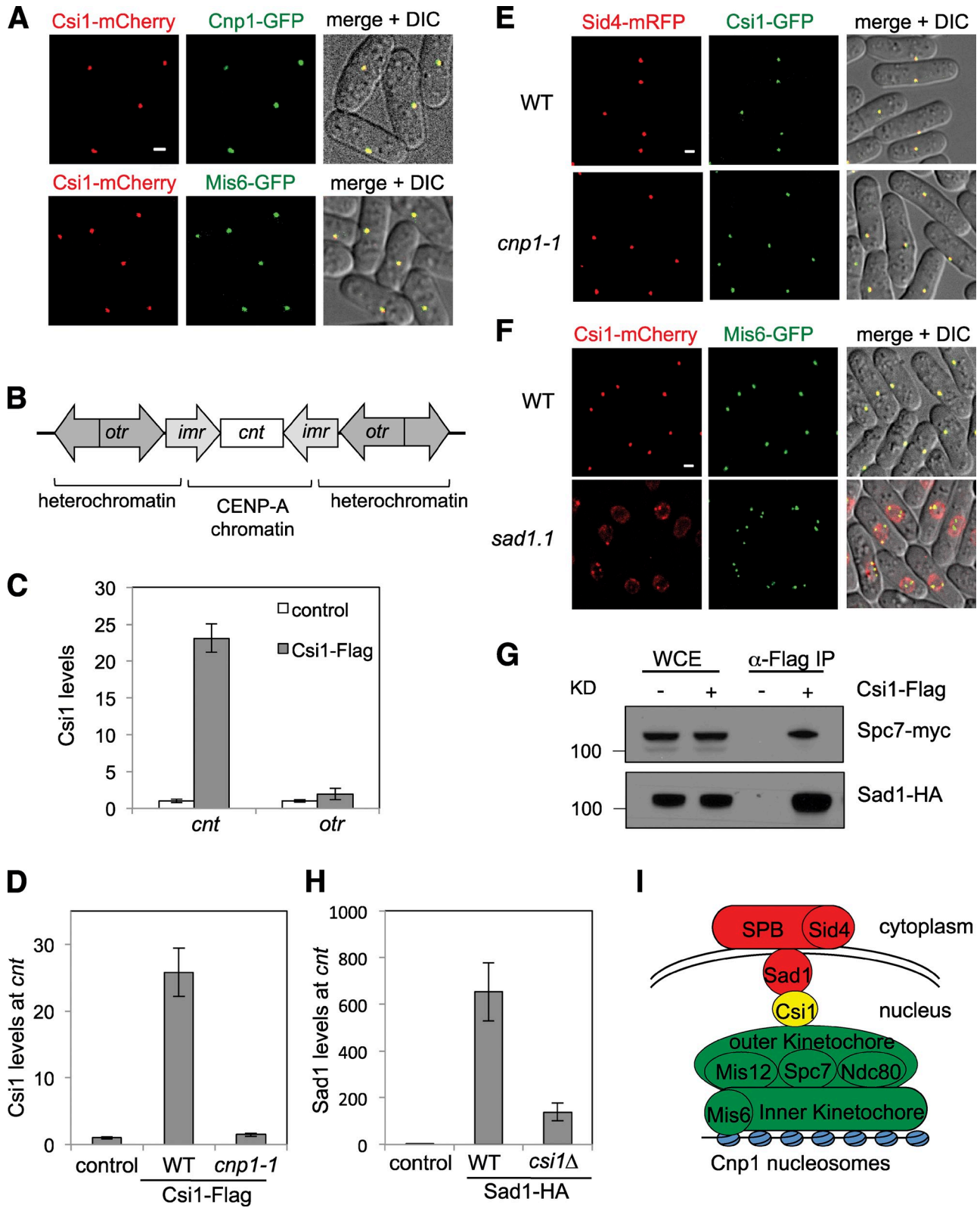

Figure 2. **Csi1 is at the SPB–kinetochore interface.** (A) Live-cell imaging of cells expressing Csi1-mCherry and indicated GFP fusions of kinetochore proteins. (B) A diagram of the fission yeast centromere region of chromosome 1. (C) ChIP analyses of Csi1-Flag levels at *cnt* and *otr*. (D) ChIP analyses of Csi1-Flag levels at *cnt*. Cells were grown at 37°C for 4 h before ChIP analysis was performed. (E) Live-cell imaging of cells expressing Csi1-GFP and Sid4-mRFP in a *cnp1-1* mutant after 4 h at 37°C. (F) Live-cell imaging of cells expressing Csi1-mCherry and Mis6-GFP in a *sad1.1* mutant after 3 h at 37°C. (G) Cell lysates from the indicated strains were immunoprecipitated with the Flag antibody to isolate Csi1-Flag. The associated proteins were detected by Western blot analyses with myc or HA antibodies. WCE, whole-cell extract. (H) ChIP analyses of Sad1-HA protein levels at *cnt*. (I) Schematic diagram of SPB–centromere organization. Error bars represent standard deviations of three experiments. DIC, differential interference contrast; IP, immunoprecipitation; WT, wild type. Bars, 1 µm.

Published November 19, 2012

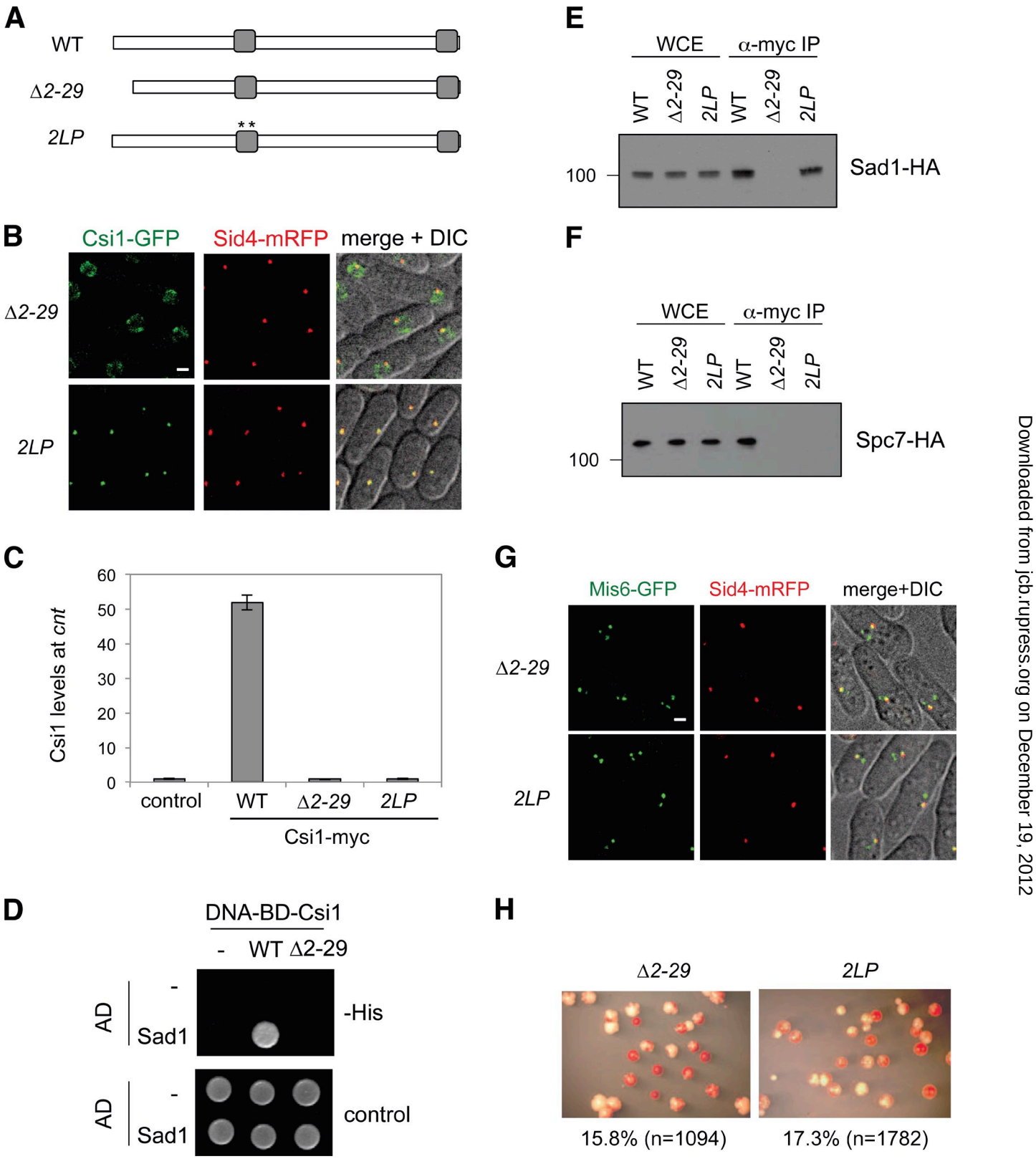

Figure 3. **Csi1 interacts with Sad1.** (A) Schematic diagrams of Csi1 and two mutants. Two asterisks represent mutations of two amino acids from L to P. (B) Live-cell imaging of mutant forms of Csi1-GFP together with Sid4-mRFP. (C) ChIP analysis of mutant Csi1 protein levels at centromeres. Error bars represent standard deviations of three experiments. (D) Yeast two-hybrid analysis of Csi1 with Sad1. Csi1 or Δ2–29 was fused with GAL4 DNA-binding domain (BD), and Sad1 was fused with an activation domain (AD). Interaction between Sad1 and Csi1 results in the activation of a *HIS3* reporter gene, allowing cells to grow in the absence of histidine. (E and F) Cell lysate from strains expressing Sad1-HA or Spc7-HA and indicated forms of Csi1-myc were immunoprecipitated with a myc antibody, and Western blot analyses were performed with a HA antibody. Molecular masses are given in kilodaltons. (G) Live-cell imaging analysis of Mis6-GFP and Sid4-mRFP in Csi1 mutants. (H) Csi1 mutant cells containing Ch16 were grown into single colonies to measure loss rate. DIC, differential interference contrast; IP, immunoprecipitation; WT, wild type. Bars, 1 μm.

Published November 19, 2012

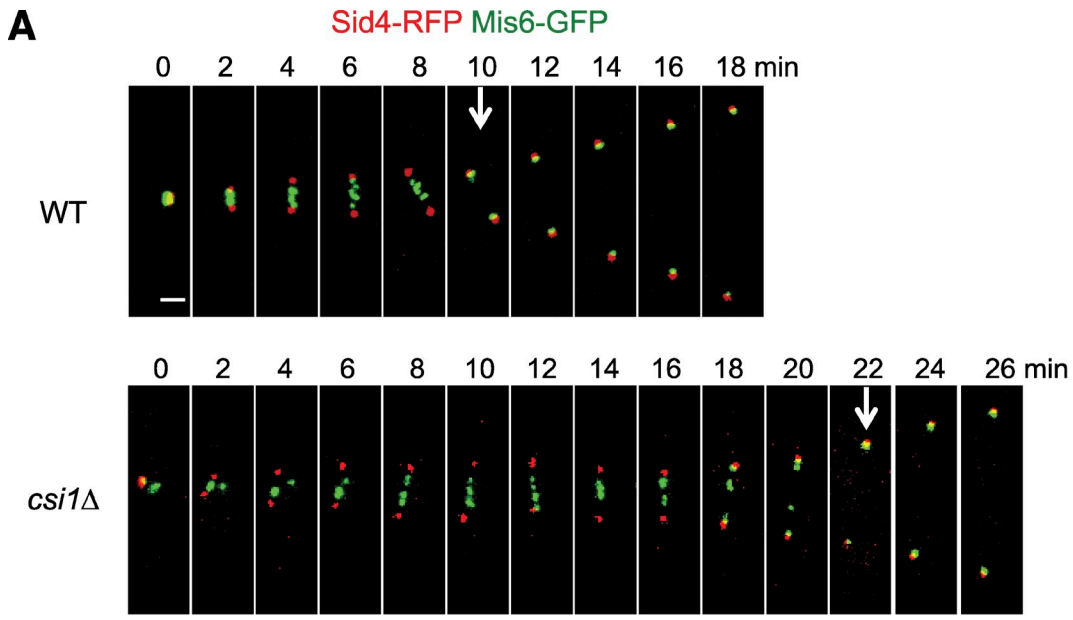

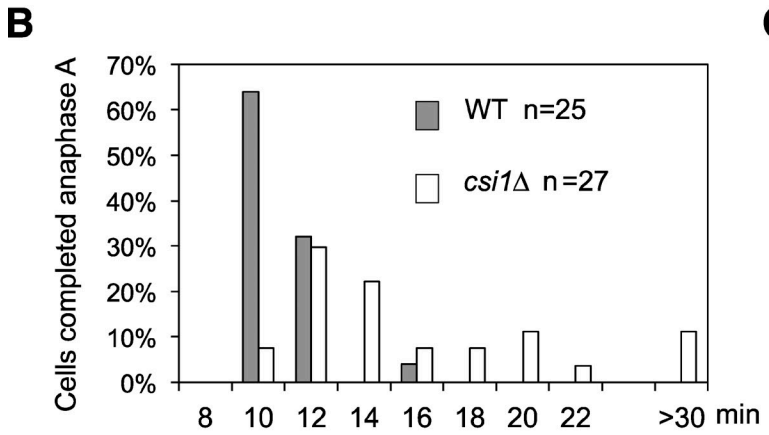

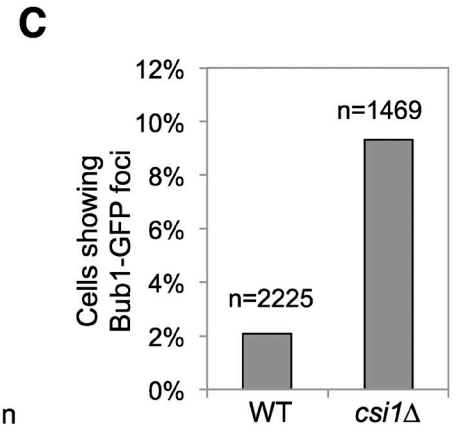

D

Csi1-SAC	
csi1Δ mph1Δ	lethal
csi1Δ bub1Δ	lethal
csi1Δ mad1Δ	lethal
csi1Δ mad2Δ	very sick
csi1Δ mad3Δ	very sick

Csi1-MAP	
csi1Δ dis1Δ	lethal
csi1Δ alp14Δ	very sick

Csi1-DASH	
csi1Δ dad1Δ	lethal
csi1Δ dad2Δ	lethal
csi1Δ dad3Δ	lethal
csi1Δ dad4Δ	lethal
csi1Δ dad5Δ	lethal
csi1Δ dam1Δ	lethal
csi1Δ ask1Δ	lethal
csi1Δ duo1Δ	lethal
csi1Δ spc19Δ	lethal
csi1Δ spc34Δ	lethal

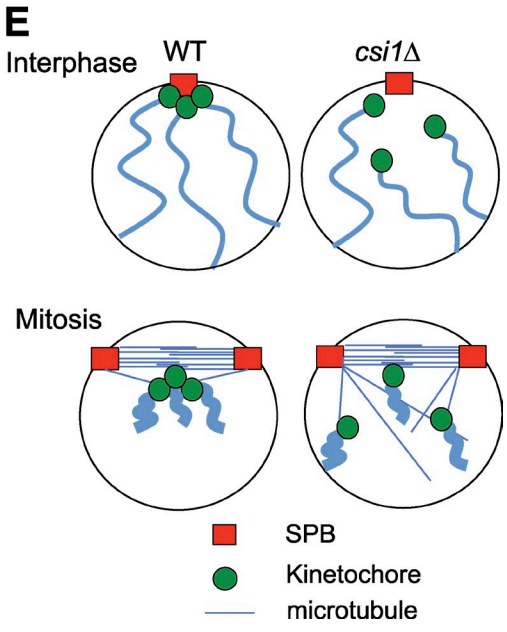

Figure 4. **Loss of Csi1 results in mitotic delays and sensitivity to perturbations in kinetochore–microtubule interactions.** (A) Time-lapse microscopy of Sid4-RFP and Mis6-GFP during mitosis. Pictures were taken at 2-min intervals. (B) The distribution of time to finish anaphase A. Time was measured from separation of SPB to the reclustering of centromeres at the SPB, indicated by arrows in A. *n* represents number of mitosis counted from a single experiment. (C) The

Published November 19, 2012

We also identified a NLS of Csi1 near its N terminus. The *csi1-ΔNLS* mutant, in which the Csi1 protein was detected only in the cytoplasm, exhibited a high rate of minichromosome loss (Fig. S3). Introducing a heterologous NLS at the C terminus restored its correct localization and rescued Ch16 maintenance defects, suggesting that Csi1 needs to be nuclear for its function. This might explain the requirement of Crm1 for centromere clustering (Funabiki et al., 1993), as Crm1 potentially regulates nuclear localization of Csi1 or other nuclear components of the SPB.

We next examined more closely the effect of Csi1 on chromosome segregation during mitosis. We used time-lapse microscopy to image cells expressing Mis6-GFP (kinetochore marker) and Sid4-mRFP (SPB marker; Fig. 4 A). We timed mitotic events relative to the separation of the two duplicated SPBs at time = 0 (Fig. 4 A). The centromeres oscillate between the two SPBs and subsequently segregate toward the SPBs during anaphase A (Funabiki et al., 1993). Wild-type cells took an average of 10.9 ± 1.4 min from SPB separation to completion of anaphase A under our experimental conditions. *csi1Δ* cells exhibited mitotic delays, with 14.6 ± 3.4 min from SPB separation to completion of anaphase A. Mis6-GFP showed a high incidence of abnormal kinetochore behavior, such as mislocalized kinetochores and lagging chromosomes, with 11% of cells failing to segregate chromosomes within 30 min (Fig. 4, A and B). The prolonged mitotic progression before anaphase suggests that the spindle assembly checkpoint (SAC) is activated (Musacchio and Salmon, 2007). Consistent with this idea, we observed a much higher percentage of *csi1Δ* cells exhibiting Bub1-GFP foci compared with wild-type cells in asynchronous cell populations (Fig. 4 C).

To further probe the function of Csi1, we examined the genetic interaction network of Csi1 via synthetic genetic array (Dixon et al., 2008; Roguev et al., 2008). Genes that showed strong negative genetic interactions confirmed by tetrad dissection analysis (Fig. 4 D) included components of the SAC, the Dam1/DASH complex (Yao and He, 2008; Buttrick and Millar, 2011), and microtubule-associated proteins Dis1 and Alp14 (XMAP215 orthologue; Nakaseko et al., 2001), all of which are located at the kinetochore–microtubule interface. The genetic interactions with SAC are consistent with our data that loss of Csi1 activates the SAC. We speculate that in the absence of SAC, cells continue mitosis with improperly attached kinetochores, resulting in missegregation of chromosomes and lethality. The DASH complex functions to couple kinetochores with microtubules (Yao and He, 2008; Buttrick and Millar, 2011) and is required for the retrieval of unattached kinetochores during mitosis (Franco et al., 2007). Without DASH, the declustered kinetochores might not be retrieved to complete chromosome segregation, leading to cell death. The genetic interactions with microtubule-associated proteins suggest that *csi1Δ* cells are very sensitive to changes in microtubule plus-end dynamics. Consistent with these findings, *csi1Δ* cells showed strong sensitivity to thiabendazole, a chemical that destabilizes microtubules (Fig. S3; Han et al., 2010).

It has been suggested that in fission yeast the clustering of centromeres during interphase allows for the rapid capture of kinetochores by intranuclear microtubules at the onset of mitosis (Fig. 4 E; Grishchuk et al., 2007), although experimental support for this model is lacking. Computational simulations of mitosis indicate that an unbiased microtubule search and capture mechanism is not efficient enough to account for mitosis in a timely manner (Wollman et al., 2005), and diverse strategies have evolved to ensure efficient capture of kinetochores by microtubules (Tanaka, 2010). For instance, in mammalian cells, centromeres are transiently arranged in a ring surrounding spindles during early prometaphase, exposing them to high concentrations of microtubules (Magidson et al., 2011). We speculated that defects in centromere clustering in Csi1 mutants contribute to delays and abnormalities in chromosome capture.

The aforementioned model predicts that increasing chromosome number would exacerbate the defects in kinetochore capture by microtubules and delay mitosis further. Indeed, when we introduced the minichromosome Ch16 into *csi1Δ* cells, the time from SPB separation to anaphase onset was longer and variable (11.2 ± 1.3 min in wild type and 18.3 ± 5.3 min in *csi1Δ* cells), with 48% of cells failing to complete mitosis within 30 min (Fig. 5, A and B). Moreover, when we introduced two minichromosomes (Ch16N and Ch16H) into *csi1Δ* cells, the cells grew very slowly and exhibited severe mitotic defects (Fig. 5 C). This effect was not a result of different kinetochore structures at the minichromosome, as the endogenous chromosome 2 also missegregated at higher rates with increasing chromosome numbers (Fig. 5 D). These results support the notion that centromere clustering contributes to proper attachment of kinetochores to microtubules during early mitosis. As centromeres need to be segregated during mitosis, we cannot artificially cluster centromeres to see whether this can rescue the mitotic delay caused by *csi1Δ*. Thus, it remains a possibility that Csi1 might also contribute to other processes that regulate mitosis.

In summary, we have identified two factors of a molecular link that attaches and clusters centromeres at the inner nuclear envelope near the SPB: the SUN domain protein Sad1, which is an inner nuclear envelope protein, and Csi1, a nuclear protein that interacts with both Sad1 and components of the kinetochore during interphase. In addition to centromere clustering defects, Csi1 mutants also exhibit prominent defects in chromosome segregation during mitosis. As Csi1 is not detectable at kinetochores during mitosis (Fig. S2 D), it is unlikely to directly mediate microtubule–kinetochore attachment. Rather, our data support a

percentage of cells showing Bub1-GFP foci in populations of asynchronously growing cells. *n* represents number of cells counted from a single experiment. (D) Genetic interaction profiles of *csi1Δ*. Tetrad dissection of individual crosses was performed to analyze genetic interactions between *csi1Δ* and other mutants. For a conclusion of lethal genetic interactions, ≥50 tetrads from each cross were dissected, and no double mutants were obtained. (E) A model showing that centromere clustering during interphase facilitates kinetochore capture by microtubules during mitosis. The clustered centromeres serve as a higher affinity platform for concerted capture by microtubules. MAP, microtubule-associated protein; WT, wild type. Bar, 1 µm.

Published November 19, 2012

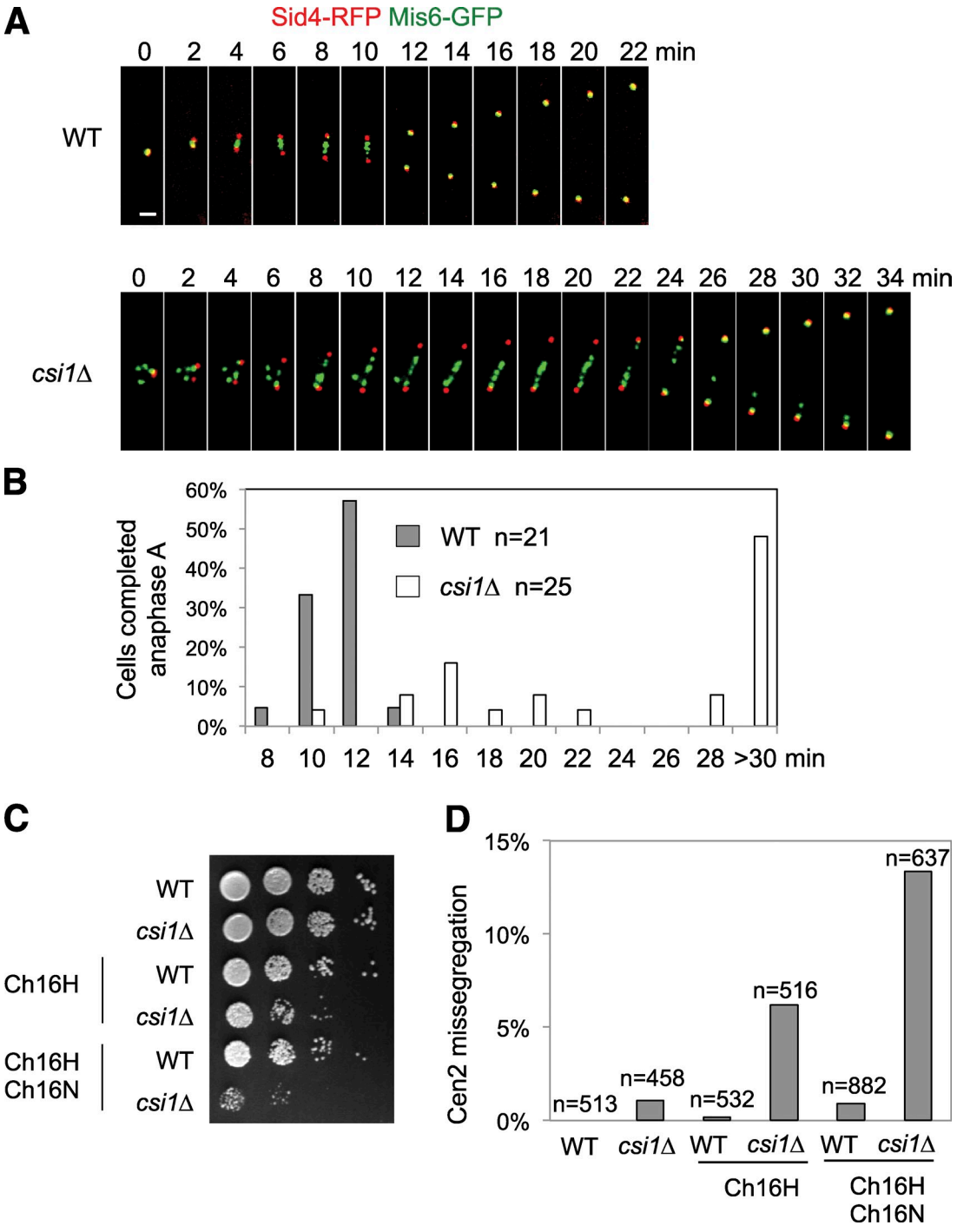

Figure 5. **Increasing chromosome number exacerbates the mitotic defects of *csi1Δ* cells.** (A) Time-lapse microscopy of Sid4-RFP and Mis6-GFP during mitosis. Both cells have Ch16. (B) The distribution of time to finish anaphase A. All cells have Ch16. *n* represents the number of mitosis counted from a single experiment. (C) Serial dilution analysis of cells containing different numbers of chromosomes. Ch16H and Ch16N are modified versions of Ch16 that confer resistance to hygromycin and nourseothricin, respectively. (D) The segregation of chromosome 2 was analyzed through microscopic examination of a strain containing a LacO array inserted near the centromere of chromosome 2 that is also expressing LacI-GFP. *n* represents the number of cells counted from a single experiment. WT, wild type. Bar, 1 µm.

model wherein Csi1-dependent centromere clustering near the SPB during interphase facilitates the capture of kinetochores by microtubules emanating from the SPBs subsequently in early mitosis. Our results highlight the importance of three-dimensional organization of the genome, which is increasingly recognized to play important regulatory roles in cellular functions.

Materials and methods

Fission yeast strains and genetic analyses

A PCR-based module method (Bähler et al., 1998) was used to construct strains expressing epitope-tagged versions of Csi1, Cnp1, Nuf2, and Cnp20 at their endogenous chromosomal location. The templates for mCherry tagging were obtained from K. Sawin (The University of Edinburgh,

Edinburgh, Scotland, UK) and the Yeast Resource Center. All mutations of Csi1 were introduced at the endogenous chromosomal locus and verified by sequencing. The majority of strains containing individual deletions were derived from the Bioneer fission yeast deletion library (Kim et al., 2010), verified via PCR, and backcrossed. Kinetochore and SPB mutants were obtained from the Japanese National BioResource Project. For serial dilution analyses, 5 µl of 10-fold dilutions of cells starting at 10^7 cells/ml were plated on the indicated medium and grown at 30°C for 3 d. To measure Ch16 loss rate, cells were spread into single colonies on medium containing low adenine (YE [yeast extract and dextrose]) to allow color development. Ch16 loss rate per generation was calculated as the number of colonies containing red half-sectors divided by the total number of colonies, which were not completely red (Hou et al., 2010). An auxin-inducible degron of IAA17 was introduced at the C terminus of Nuf2 at its endogenous chromosomal locus in a strain containing the plant F-box protein TIR1 fused with fission yeast protein Skp1 (Kanke et al., 2011). Cells were grown in medium containing 300 µg/ml napthaleneacetic acid for 6 h to inactivate Nuf2.

Live-cell imaging

Live-cell imaging was performed as described previously (Tran et al., 2004). Cells were grown in Edinburgh minimal medium (EMM) to reach mid-log phase and mounted on EMM-agar pads. Images were taken at 25°C unless otherwise noted with an inverted microscope (Eclipse Ti; Nikon) equipped with a 100×, 1.4 NA objective, spinning-disc confocal head (CSU10; Yokagawa Corporation of America), and an EM charge-coupled device camera (ImagEM; Hamamatsu Photonics). Images were acquired with NIS-Elements (Nikon) with z stacks at 0.4-µm intervals and then flattened. ImageJ (National Institutes of Health) was used for image analysis. For time-lapse microscopy, images were taken every 2 min.

ChIP analysis

ChIP analyses were performed as described previously (Hou et al., 2010). In brief, mid-log phase cells were cross-linked with freshly made 3% paraformaldehyde, and cell lysates were prepared by vigorously shaking with glass beads using a bead beater. The cleared lysates were sonicated to generate an average DNA fragment size between 0.5 and 1 kb. The following antibodies Flag (Sigma-Aldrich), HA (12CA5), and myc (Sigma-Aldrich) were used for immunoprecipitation. Quantitative real-time PCR was performed with SYBR green quantitative PCR master mix (Maxima; Fermentas) in a real-time PCR system (ABI 7300; Applied Biosystems). DNA serial dilutions were used as templates to generate a standard curve of amplification for each pair of primers, and the relative concentration of target sequence was calculated accordingly. An *act1* fragment was used as a reference to calculate the enrichment of ChIP over whole-cell extract for each target sequence. The high enrichment value of Sad1 at centromeres is a result of the low background of the HA antibody used.

Yeast two-hybrid assay

Csi1 and Csi1-(Δ2–29) were cloned into pGTB9 (Takara Bio Inc.) to generate fusion with the GAL4 DNA-binding domain. Sad1 was cloned into pGAD424 (Takara Bio Inc.) to generate fusion with the GAL4 activation domain. Both plasmids were transformed into the budding yeast strain pJ69-4A (James et al., 1996), and transformants were selected on medium lacking tryptophan and leucine to maintain both plasmids. The interaction of two proteins was indicated by the activation of a *HIS3* reporter, allowing growth on medium lacking histidine.

Coimmunoprecipitation analysis

2 liters of mid-log phase cells were collected and washed with 2× HC buffer (300 mM Hepes-KOH, pH 7.6, 2 mM EDTA, 100 mM KCl, 20% glycerol, 2 mM DTT, and protease inhibitor cocktail [Roche]) before frozen into small nuggets with liquid nitrogen. The frozen yeast cells were mixed with dry ice and vigorously blended using a household blender. The resulting cell lysates were incubation with HC buffer containing 150 mM KCl for 30 min and centrifuged at 82,700 *g* for 3 h. Immunoprecipitation was performed by incubating cell lysates with Flag or myc antibody for 4 h followed by incubation with protein G–agarose beads for an hour. The beads were washed four times with HC containing 150 mM KCl. Western blot analyses were performed with myc or HA antibodies.

Assay of endogenous chromosome 2 segregation

Mid-log phase cells were resuspended in EMM medium containing 50 µg/ml calcofluor before image acquisition. LacI-GFP tethered to a tandem LacO array was used to measure centromere 2, and calcofluor-stained septins indicate cells that recently completed division. The number of cells with missegregated centromere 2 (two GFP foci in one daughter cell and no GFP focus in the other) was quantified.

SAC activation assay

Cells containing Bub1-GFP were grown in EMM medium until mid-log phase and fixed with 2% formaldehyde in 0.1 M phosphate buffer, pH 7.4, before image acquisition.

Online supplemental material

Fig. S1 shows that Csi1 is not required for the localization of kinetochore protein Cnp20 or SPB protein Sad1. Fig. S2 shows that Csi1 localization to centromeres is dependent on the presence of functional kinetochores, and this localization is cell cycle dependent. Fig. S3 shows that Csi1 is a nuclear protein, and nuclear localization is required for Csi1 function. Online supplemental material is available at http://www.jcb.org/cgi/content/full/jcb.201208001/DC1.

We thank Silvere Pagant for technical advice, the Japanese National BioResource Project, Michael Keogh, Ken Sawin, and Yeast Resource Center for yeast strains and reagents, Bharat Reddy for helpful discussions, Meehan Crist and Allison Cohen for editorial assistance, and James Manley for critical reading of the manuscript.

This work is supported by National Institutes of Health grants R01-GM085145 to S. Jia, R01-GM069670 to F. Chang, and R01-GM078186 and R01-GM085089 to E.A. Miller. S.P. Kallgren is supported by National Institutes of Health training grant T32-GM008798.

Submitted: 3 August 2012
Accepted: 19 October 2012

References

Appelgren, H., B. Kniola, and K. Ekwall. 2003. Distinct centromere domain structures with separate functions demonstrated in live fission yeast cells. *J. Cell Sci.* 116:4035–4042. http://dx.doi.org/10.1242/jcs.00707

Asakawa, H., A. Hayashi, T. Haraguchi, and Y. Hiraoka. 2005. Dissociation of the Nuf2-Ndc80 complex releases centromeres from the spindle-pole body during meiotic prophase in fission yeast. *Mol. Biol. Cell*. 16:2325–2338. http://dx.doi.org/10.1091/mbc.E04-11-0996

Bähler, J., J.Q. Wu, M.S. Longtine, N.G. Shah, A. McKenzie III, A.B. Steever, A. Wach, P. Philippsen, and J.R. Pringle. 1998. Heterologous modules for efficient and versatile PCR-based gene targeting in *Schizosaccharomyces pombe*. *Yeast*. 14:943–951. http://dx.doi.org/10.1002/(SICI)1097-0061(199807)14:10<943::AID-YEA292>3.0.CO;2-Y

Buttrick, G.J., and J.B. Millar. 2011. Ringing the changes: emerging roles for DASH at the kinetochore-microtubule interface. *Chromosome Res.* 19:393–407. http://dx.doi.org/10.1007/s10577-011-9185-8

Buttrick, G.J., J.C. Meadows, T.C. Lancaster, V. Vanoosthuyse, L.A. Shepperd, K.L. Hoe, D.U. Kim, H.O. Park, K.G. Hardwick, and J.B. Millar. 2011. Nsk1 ensures accurate chromosome segregation by promoting association of kinetochores to spindle poles during anaphase B. *Mol. Biol. Cell*. 22:4486–4502. http://dx.doi.org/10.1091/mbc.E11-07-0608

Castagnetti, S., S. Oliferenko, and P. Nurse. 2010. Fission yeast cells undergo nuclear division in the absence of spindle microtubules. *PLoS Biol.* 8: e1000512. http://dx.doi.org/10.1371/journal.pbio.1000512

Chang, L., and K.L. Gould. 2000. Sid4p is required to localize components of the septation initiation pathway to the spindle pole body in fission yeast. *Proc. Natl. Acad. Sci. USA*. 97:5249–5254. http://dx.doi.org/10.1073/pnas.97.10.5249

Cheeseman, I.M., and A. Desai. 2008. Molecular architecture of the kinetochore-microtubule interface. *Nat. Rev. Mol. Cell Biol.* 9:33–46. http://dx.doi.org/10.1038/nrm2310

Chen, J.S., L.X. Lu, M.D. Ohi, K.M. Creamer, C. English, J.F. Partridge, R. Ohi, and K.L. Gould. 2011. Cdk1 phosphorylation of the kinetochore protein Nsk1 prevents error-prone chromosome segregation. *J. Cell Biol.* 195:583–593. http://dx.doi.org/10.1083/jcb.201105074

Chikashige, Y., C. Tsutsumi, M. Yamane, K. Okamasa, T. Haraguchi, and Y. Hiraoka. 2006. Meiotic proteins bqt1 and bqt2 tether telomeres to form the bouquet arrangement of chromosomes. *Cell*. 125:59–69. http://dx.doi.org/10.1016/j.cell.2006.01.048

Ding, R., R.R. West, D.M. Morphew, B.R. Oakley, and J.R. McIntosh. 1997. The spindle pole body of *Schizosaccharomyces pombe* enters and leaves the nuclear envelope as the cell cycle proceeds. *Mol. Biol. Cell*. 8: 1461–1479.

Dixon, S.J., Y. Fedyshyn, J.L. Koh, T.S. Prasad, C. Chahwan, G. Chua, K. Toufighi, A. Baryshnikova, J. Hayles, K.L. Hoe, et al. 2008. Significant conservation of synthetic lethal genetic interaction networks between distantly related eukaryotes. *Proc. Natl. Acad. Sci. USA*. 105:16653–16658. http://dx.doi.org/10.1073/pnas.0806261105

Fang, Y., and D.L. Spector. 2005. Centromere positioning and dynamics in living *Arabidopsis* plants. *Mol. Biol. Cell*. 16:5710–5718. http://dx.doi.org/10.1091/mbc.E05-08-0706

Franco, A., J.C. Meadows, and J.B. Millar. 2007. The Dam1/DASH complex is required for the retrieval of unclustered kinetochores in fission yeast. *J. Cell Sci.* 120:3345–3351. http://dx.doi.org/10.1242/jcs.013698

Fukuda, M., S. Asano, T. Nakamura, M. Adachi, M. Yoshida, M. Yanagida, and E. Nishida. 1997. CRM1 is responsible for intracellular transport mediated by the nuclear export signal. *Nature*. 390:308–311. http://dx.doi.org/10.1038/36894

Funabiki, H., I. Hagan, S. Uzawa, and M. Yanagida. 1993. Cell cycle-dependent specific positioning and clustering of centromeres and telomeres in fission yeast. *J. Cell Biol.* 121:961–976. http://dx.doi.org/10.1083/jcb.121.5.961

Grishchuk, E.L., I.S. Spiridonov, and J.R. McIntosh. 2007. Mitotic chromosome biorientation in fission yeast is enhanced by dynein and a minus-end-directed, kinesin-like protein. *Mol. Biol. Cell*. 18:2216–2225. http://dx.doi.org/10.1091/mbc.E06-11-0987

Hagan, I., and M. Yanagida. 1995. The product of the spindle formation gene *sad1*$^{+}$ associates with the fission yeast spindle pole body and is essential for viability. *J. Cell Biol.* 129:1033–1047. http://dx.doi.org/10.1083/jcb.129.4.1033

Han, T.X., X.Y. Xu, M.J. Zhang, X. Peng, and L.L. Du. 2010. Global fitness profiling of fission yeast deletion strains by barcode sequencing. *Genome Biol.* 11:R60. http://dx.doi.org/10.1186/gb-2010-11-6-r60

Hiraoka, Y., H. Maekawa, H. Asakawa, Y. Chikashige, T. Kojidani, H. Osakada, A. Matsuda, and T. Haraguchi. 2011. Inner nuclear membrane protein Ima1 is dispensable for intranuclear positioning of centromeres. *Genes Cells*. 16:1000–1011. http://dx.doi.org/10.1111/j.1365-2443.2011.01544.x

Hou, H., Y. Wang, S.P. Kallgren, J. Thompson, J.R. Yates III, and S. Jia. 2010. Histone variant H2A.Z regulates centromere silencing and chromosome segregation in fission yeast. *J. Biol. Chem.* 285:1909–1918. http://dx.doi.org/10.1074/jbc.M109.058487

James, P., J. Halladay, and E.A. Craig. 1996. Genomic libraries and a host strain designed for highly efficient two-hybrid selection in yeast. *Genetics*. 144:1425–1436.

Jin, Q., E. Trelles-Sticken, H. Scherthan, and J. Loidl. 1998. Yeast nuclei display prominent centromere clustering that is reduced in nondividing cells and in meiotic prophase. *J. Cell Biol.* 141:21–29. http://dx.doi.org/10.1083/jcb.141.1.21

Kanke, M., K. Nishimura, M. Kanemaki, T. Kakimoto, T.S. Takahashi, T. Nakagawa, and H. Masukata. 2011. Auxin-inducible protein depletion system in fission yeast. *BMC Cell Biol.* 12:8. http://dx.doi.org/10.1186/1471-2121-12-8

Kim, D.U., J. Hayles, D. Kim, V. Wood, H.O. Park, M. Won, H.S. Yoo, T. Duhig, M. Nam, G. Palmer, et al. 2010. Analysis of a genome-wide set of gene deletions in the fission yeast *Schizosaccharomyces pombe*. *Nat. Biotechnol.* 28:617–623. http://dx.doi.org/10.1038/nbt.1628

King, M.C., T.G. Drivas, and G. Blobel. 2008. A network of nuclear envelope membrane proteins linking centromeres to microtubules. *Cell*. 134:427–438. http://dx.doi.org/10.1016/j.cell.2008.06.022

Magidson, V., C.B. O'Connell, J. Lončarek, R. Paul, A. Mogilner, and A. Khodjakov. 2011. The spatial arrangement of chromosomes during prometaphase facilitates spindle assembly. *Cell*. 146:555–567. http://dx.doi.org/10.1016/j.cell.2011.07.012

Meister, P., S.E. Mango, and S.M. Gasser. 2011. Locking the genome: nuclear organization and cell fate. *Curr. Opin. Genet. Dev.* 21:167–174. http://dx.doi.org/10.1016/j.gde.2011.01.023

Mekhail, K., and D. Moazed. 2010. The nuclear envelope in genome organization, expression and stability. *Nat. Rev. Mol. Cell Biol.* 11:317–328. http://dx.doi.org/10.1038/nrm2894

Misteli, T. 2007. Beyond the sequence: cellular organization of genome function. *Cell*. 128:787–800. http://dx.doi.org/10.1016/j.cell.2007.01.028

Musacchio, A., and E.D. Salmon. 2007. The spindle-assembly checkpoint in space and time. *Nat. Rev. Mol. Cell Biol.* 8:379–393. http://dx.doi.org/10.1038/nrm2163

Nakaseko, Y., G. Goshima, J. Morishita, and M. Yanagida. 2001. M phase-specific kinetochore proteins in fission yeast: microtubule-associating Dis1 and Mtc1 display rapid separation and segregation during anaphase. *Curr. Biol.* 11:537–549. http://dx.doi.org/10.1016/S0960-9822(01)00155-5

Niwa, O., T. Matsumoto, and M. Yanagida. 1986. Construction of a mini-chromosome by deletion and its mitotic and meiotic behaviour in fission yeast. *Mol. Genet. Genomics*. 203:397–405. http://dx.doi.org/10.1007/BF00422063

Rajapakse, I., and M. Groudine. 2011. On emerging nuclear order. *J. Cell Biol.* 192:711–721. http://dx.doi.org/10.1083/jcb.201010129

Razafsky, D., and D. Hodzic. 2009. Bringing KASH under the SUN: the many faces of nucleo-cytoskeletal connections. *J. Cell Biol.* 186:461–472. http://dx.doi.org/10.1083/jcb.200906068

Roguev, A., S. Bandyopadhyay, M. Zofall, K. Zhang, T. Fischer, S.R. Collins, H. Qu, M. Shales, H.O. Park, J. Hayles, et al. 2008. Conservation and rewiring of functional modules revealed by an epistasis map in fission yeast. *Science*. 322:405–410. http://dx.doi.org/10.1126/science.1162609

Starr, D.A., and J.A. Fischer. 2005. KASH 'n Karry: the KASH domain family of cargo-specific cytoskeletal adaptor proteins. *Bioessays*. 27:1136–1146. http://dx.doi.org/10.1002/bies.20312

Takahashi, K., S. Murakami, Y. Chikashige, H. Funabiki, O. Niwa, and M. Yanagida. 1992. A low copy number central sequence with strict symmetry and unusual chromatin structure in fission yeast centromere. *Mol. Biol. Cell*. 3:819–835.

Tanaka, T.U. 2010. Kinetochore-microtubule interactions: steps towards bi-orientation. *EMBO J.* 29:4070–4082. http://dx.doi.org/10.1038/emboj.2010.294

Tran, P.T., A. Paoletti, and F. Chang. 2004. Imaging green fluorescent protein fusions in living fission yeast cells. *Methods*. 33:220–225. http://dx.doi.org/10.1016/j.ymeth.2003.11.017

Verdaasdonk, J.S., and K. Bloom. 2011. Centromeres: unique chromatin structures that drive chromosome segregation. *Nat. Rev. Mol. Cell Biol.* 12:320–332. http://dx.doi.org/10.1038/nrm3107

Wollman, R., E.N. Cytrynbaum, J.T. Jones, T. Meyer, J.M. Scholey, and A. Mogilner. 2005. Efficient chromosome capture requires a bias in the 'search-and-capture' process during mitotic-spindle assembly. *Curr. Biol.* 15:828–832. http://dx.doi.org/10.1016/j.cub.2005.03.019

Yao, J., and X. He. 2008. Kinetochore assembly: building a molecular machine that drives chromosome movement. *Mol. Biosyst.* 4:987–992. http://dx.doi.org/10.1039/b719627j